ACS Catalysis

Article

Chemoselective Catalytic Dehydrogenative Cross Coupling of 2-Acylimidazoles: Mechanistic Investigations and Synthetic Scope

Tsukushi Tanaka, Kayoko Hashiguchi, Takafumi Tanaka, Ryo Yazaki, and Takashi Ohshima

ACS Catal., **Just Accepted Manuscript** • Publication Date (Web): 30 Jul 2018

ACS Publications

is published by the American Chemical Society. 1155 Sixteenth Street N.W., Washington, DC 20036

Chemoselective Catalytic Dehydrogenative Cross Coupling of 2-Acylimidazoles: Mechanistic Investigations and Synthetic Scope

Tsukushi Tanaka, Kayoko Hashiguchi, Takafumi Tanaka, Ryo Yazaki* and Takashi Ohshima*

Graduate School of Pharmaceutical Sciences, Kyushu University, Maidashi, Higashi-ku, Fukuoka 812-8582 Japan

ABSTRACT: Chemoselective iron-catalyzed dehydrogenative cross-coupling using 2-acylimidazoles is described. The addition of a phosphine oxide ligand substantially facilitated the generation of *tert*-butoxy radicals from di-*tert*-butyl peroxide, allowing for efficient benzylic C–H bond cleavage under mild conditions. Extensive mechanistic studies revealed that the enolization of 2-acylimidazole proceeded through dual iron catalyst activation, followed by subsequent chemoselective cross-coupling with a benzyl radical over an undesired benzyl radical-derived homo-coupling dimer that inevitably formed in earlier reported conditions. A variety of alkylarenes, aliphatic alkane and functionalized 2-acylimidazoles were applicable, demonstrating the synthetic utility of the present catalysis. Contiguous all-carbon quaternary carbons were constructed through dehydrogenative cross-coupling. The catalytic chemoselective activation of 2-acylimidazole over bidentate coordinative and much more acidic malonate diester was particular noteworthy. Catalytic oxidative cross-enolate coupling of two distinct carboxylic acid equivalents was also achieved using acetonitrile as a coupling partner.

Keywords: redox catalysis, Lewis acid, C-H activation, dehydrogenative, dual iron activation, hydrocarbon, α-alkylation, quaternary carbon center

Introduction

Inert C–H bond transformation to a C–C bond is considered an ideal process for constructing carbon frameworks in terms of atom- and step-economy.[1] Abundant hydrocarbon feedstock, such as toluene derivatives and alkanes, is a highly attractive starting material for sp^3 C–H bond functionalization. Transformation of an sp^3 C–H bond to a C–C bond, however, remains a significant challenge in modern organic chemistry compared to the transformation of an sp^2 C–H bond due to the lack of a coordinating π-bond.[2] Due to the intrinsic low acidity of the sp^3 C–H bonds of hydrocarbon feedstock, deprotonative activation by Brønsted bases alone is quite difficult.[3] On the other hand, a radical process is considered an efficient activation mode for sp^3 C–H bond functionalization,[4] but the radical process generates extremely reactive transient radical species and these radical species easily couple with each other, thereby providing undesired homo-coupling dimers as major products.[5] Therefore, olefins, aromatics, and organometallic reagents as an activated form are generally utilized as coupling partners to readily capture the transient radicals generated over undesired homo-coupling dimer formation derived from transient radicals (Scheme 1A).[6-8] On the other hand, coupling an sp^3 carbon with transient radicals is a formidable challenge because efficient in-situ activation such as deprotonation may be required to avoid generating a significant amount of homo-coupling dimers derived from the transient radicals (Scheme 1B).[8] Recently, Chatani's and You's groups reported elegant directing group-assisted strategies for dehydrogenative cross-coupling reactions to generate in-situ catalytic active species.[9,10] These reactions required a high temperature, however, presumably to efficiently generate transient radicals derived from alkylarenes (thermal radical generation) (Scheme 1C).

Alkylation of carbonyls is one of the most fundamental and well-established Csp^3–Csp^3 bond-forming transformations.[11] In general, alkylation of carbonyls is performed using alkyl halide with stoichiometric amounts of strong bases such as lithium diisopropylamide for activating carbonyls. This conventional method, however, has several drawbacks. 1) Basic conditions limit the functional group tolerance and chemoselective deprotonative activation of less acidic carbonyls over more acidic carbonyls.[12] 2) Alkyl halides must be prepared.[13] For example, benzyl bromide is commonly prepared from toluene with bromine or *N*-bromo succinimide. 3) Sterically-hindered substrates are difficult to use. Especially, constructing a contiguous all-carbon quaternary carbon center is quite challenging.[14] In contrast, dehydrogenative C–C bond formation of carbonyls with hydrocarbon feedstock is an ideal process. Li's pioneering work was performed using tautomerizable 1,3-diketones with diarylmethane derivatives.[15] Several examples were recently reported using hydrocarbon feedstock as an alkylating reagent for coupling with carbonyls.[16] These reported reactions, however, require the use of tautomerizable carbonyls, 1.3-diketones or 1,3-ketoesters, to rapidly capture the transient radicals (Scheme 1A).[17] Moreover, high temperature is needed to generate radical species and most cases suffered from the homo-coupling formation of hydrocarbon, resulting in only a moderate chemical yield.[16d,17] Herein we developed a catalytic dehydrogenative Csp^3–Csp^3 bond-forming reaction using hydrocarbon feedstock with non-tautomerizable

2-acylimidazole under mild conditions (Scheme 1D).[18,19] Notably, we observed only a trace amount of the undesired homo-coupling dimer derived from hydrocarbon feedstock. Extensive mechanistic studies revealed that ligand addition substantially facilitated the generation of *tert*-butoxy radicals from di-*tert*-bulyl peroxide (DTBP), allowing for catalyst-controlled transient radical generation from feedstock hydrocarbon. In addition, dual activation of 2-acylimidazoles by an iron catalyst occurred for efficient enolization.

Scheme 1. Radical Process for C-H to C-C Transformation

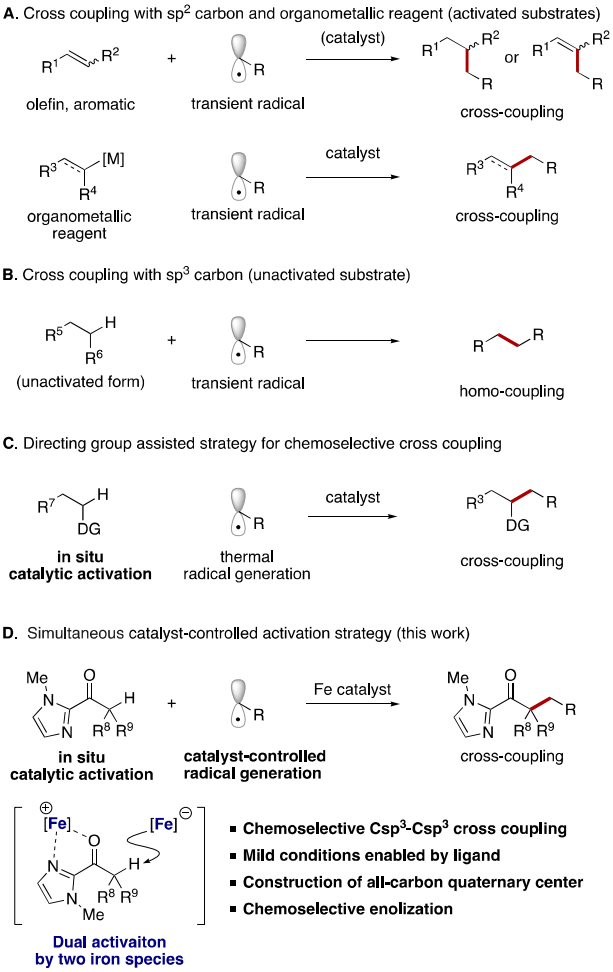

Results and Discussion

1. Development of Iron-Catalyzed Dehydrogenative Coupling of 2-Acylimidazole with Toluene

We began our investigation using 2-acylimidazole **1a** as an enolate precursor in toluene (**2a**) with $FeCl_3$ and DTBP at 120 °C (Table 1). A low chemical yield was observed without the ligand (entry 1). Pyridine derivatives considerably facilitated the reaction and benzylated product **3aa** was produced in moderate yield (entries 2–4). Pyridine oxide (**L4**) was not effective for the present catalysis (entry 5). Next, we investigated monophosphine ligands (entries 6–8). Among them, **L7** afforded product **3aa** in high yield. To confirm the effectiveness of the monodentate ligands, we evaluated several bidentate ligands (entries 9–11). *N*,*N*-ligand, 2,2'-bipyridyl (**L8**), 1,10-phenanthroline (**L9**), and BINAP (**L10**) afforded product **3aa** in only low chemical yield. These results led us to further

Table 1. Conditions Screening[a]

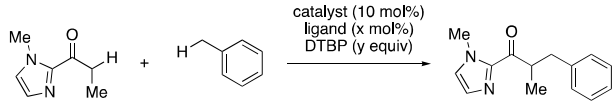

entry	catalyst	ligand (x mol%)	DTBP (y equiv)	temp. (°C)	time (h)	yield (%)
1	$FeCl_3$	—	3.3	120	4	10
2	$FeCl_3$	**L1** (20)	3.3	120	4	65
3	$FeCl_3$	**L2** (20)	3.3	120	4	59
4	$FeCl_3$	**L3** (20)	3.3	120	4	57
5	$FeCl_3$	**L4** (20)	3.3	120	4	14
6	$FeCl_3$	**L5** (20)	3.3	120	4	67
7	$FeCl_3$	**L6** (20)	3.3	120	4	31
8	$FeCl_3$	**L7** (20)	3.3	120	4	74
9	$FeCl_3$	**L8** (10)	3.3	120	4	5
10	$FeCl_3$	**L9** (10)	3.3	120	4	1
11	$FeCl_3$	**L10** (10)	3.3	120	4	28
12	$FeCl_3$	**L7** (5)	3.3	120	4	73
13	$FeCl_3$	**L7** (10)	3.3	120	4	74
14	$FeCl_3$	**L7** (20)	3.3	120	4	74
15	$FeCl_3$	**L7** (30)	3.3	120	4	61
16	$FeCl_3$	**L7** (10)	3.3	80	18	79
17	$FeCl_3$	**L7** (10)	1.7	80	8	79
18	$FeCl_3$	**L11** (10)	1.7	80	8	74
19	$FeCl_2$	**L11** (10)	1.7	80	8	85 (83)[b]
20	$FeCl_2$	**L7** (10)	1.7	80	8	74
21	$FeCl_2$	**L11** (2.5)	1.7	80	24	80
22[c]	$FeCl_2$	**L11** (10)	1.7	80	24	76

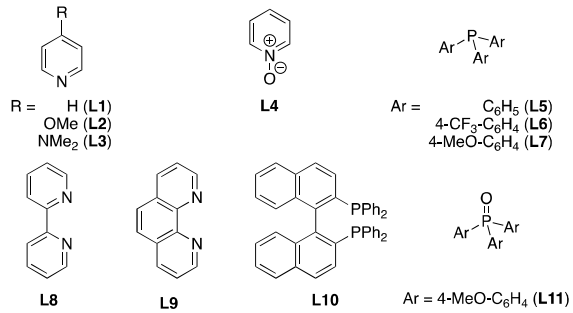

[a]Conditions: **1a** (0.23 mmol), **2a** (1.14 ml, 47 equiv). Yields were determined by ^{1}H-NMR analysis using 1,2,4,5-Tetramethylbenzene as an internal standard. [b]Isolated yield was shown. [c]A mixture of toluene (0.49 ml, 20 equiv) and benzene (0.65 ml, 0.20 M) was used.

investigate the optimal amount of ligand **L7** (entries 12–15). Although a range of 5-20 mol% of the ligand did not affect the

chemical yield, 30 mol% ligand decreased the yield. To demonstrate the mildness of the present catalysis, the reaction was performed under lower temperature. Previous catalytic dehydrogenative cross-coupling reactions of toluene derivatives were generally performed at temperatures higher than 120 °C.[20] In contrast, our catalysis can be performed at 80 °C, and product **3aa** was observed in 79% yield with a prolonged reaction time (entry 16). In addition, the amount of DTBP was reduced to 1.7 equivalents with no detrimental effects (entry 17). During the reaction optimization process, we found that **L7** was completely oxidized to phosphine oxide **L11** within several minutes based on crude ^{31}P-NMR, indicating that the actual ligand was **L11**.Thus, we evaluated **L11** as a ligand. We envisioned that Fe(III) species would be reduced to afford Fe(II) species followed by Fenton-type reaction, generating *tert*-butyoxy radical and ^{t}BuO-Fe(III) species. Thus we also investigate $FeCl_2$ as a catalyst. Although combined use with $FeCl_3$ afforded a yield comparable to that obtained using **L7** (entry 18), the $FeCl_2$-**L11** system exhibited superior catalytic performance, and the desired product was isolated in 83% yield (entry 19). It is noteworthy that only a trace amount of dibenzyl, an undesired homo-coupling product of toluene (**2a**), was observed under the optimized conditions (entry 19), while some dibenzyl was observed at 120 °C. The combination of $FeCl_2$ with **L7** was less effective (entry 20). Ligand could be reduced to 2.5 mol% without significant loss of the chemical yield (entry 21). Benzene could be used as a co-solvent and product **3aa** was observed in 76% yield using 20 equivalents of toluene (entry 22).

As control experiments, each component was omitted from the standard conditions (Table 2). No product was observed in the absence of **L11** or $FeCl_2$ (entries 2 and 3). DTBP was also essential for promoting the reaction, presumably to generate the benzyl radical (entry 4).[21] Single use of each component was also ineffective for promoting the reaction (entries 5–7). Although the reaction was not promoted at 80 °C in the absence of **L11** (entry 3), moderate yield was observed at 120 °C, a temperature at which the *tert*-butoxy radical would not be generated by heating without the assistance of $FeCl_2$/**L11**. These results indicated that $FeCl_2$/**L11** facilitated the homolytic cleavage of DTBP, generating *tert*-butoxy radicals at low temperature. The superiority of **L11** was further confirmed by the reaction at 80 °C (entries 9 and 10).

Table 2. Control Experiments[a]

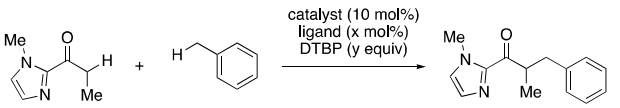

entry	catalyst	ligand (x mol%)	DTBP (y equiv)	temp. (°C)	time (h)	yield (%)
1	$FeCl_2$	**L11** (10)	1.7	80	8	85
2	—	**L11** (10)	1.7	80	8	N.D.
3	$FeCl_2$	—	1.7	80	8	N.D.
4	$FeCl_2$	**L11** (10)	—	80	8	N.D.
5	$FeCl_2$	—	—	80	8	N.D.
6	—	**L11** (10)	—	80	8	N.D.
7	—	—	1.7	80	8	N.D.
8	$FeCl_2$	—	1.7	120	8	55
9	$FeCl_2$	**L3** (10)	1.7	80	8	28
10	$FeCl_2$	**L12** (10)	1.7	80	8	7

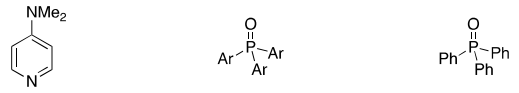

[a]Conditions: **1a** (0.23 mmol), **2a** (1.14 ml, 47 equiv). Yields were determined by ^{1}H-NMR analysis using 1,2,4,5-Tetramethylbenzene as an internal standard.

2. Mechanistic Studies

2-1. Elucidation of the Role of Ligand

To check the effect of Lewis base, Lewis basic product **3aa** was added to the reaction conditions using *p*-xylene (**2b**) as a substrate without **L11** at 120 °C (Scheme 2a). In the absence of **3aa**, product **3ab** was produced in 4% yield after stirring for 1 h. In the presence of 1.0 equivalent of **3aa**, the yield increased, indicating that Lewis basic **3aa** also facilitated the reaction rate and no catalyst deactivation by product **3aa** occurred. Next, we evaluated **3aa** and **L11** as a ligand to facilitate the reaction rate at lower reaction temperature (Scheme 2b). Although 10 mol% **3aa** facilitated the reaction (0% yield vs 36% yield), **L11** was a more effective ligand, affording product **3ab** in 92% yield.

Scheme 2. Effect of Lewis Bases

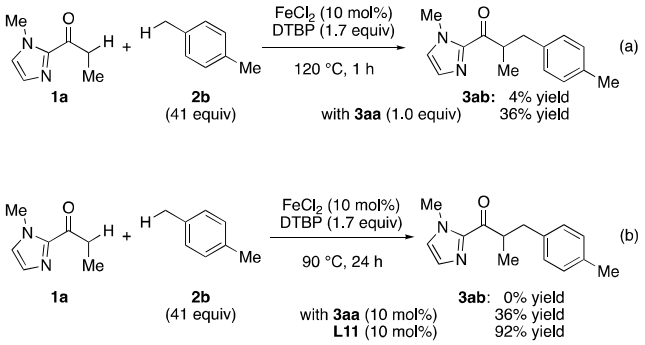

Next, we investigated the Lewis base effect of the C–H bond cleavage of toluene (Scheme 3). Without $FeCl_2$ and **L11**, no homo-coupling dimer **4** was observed at 80 °C. On the other hand, **4** was detected at 120 °C, suggesting that *tert*-butoxy radicals could be thermally generated at 120 °C (Scheme 3a). In the presence of $FeCl_2$ at 80 °C, no homo-coupling dimer **4** was observed. In sharp contrast, homo-coupling dimer **4** was observed in the presence of both $FeCl_2$ and **L11**, indicating that $FeCl_2$/**L11** facilitated the generation of *tert*-butoxy radicals through a Fenton-type reaction (Scheme 3).[22] We also confirmed that in the absence of $FeCl_2$, no homo-coupling dimer **4** was observed using **L11** and DTBP, indicating that the combined use of $FeCl_2$ and **L11** efficiently controls the generation of *tert*-butoxy radicals.

Scheme 3. Effect of Lewis Bases in C-H Bond Cleavage

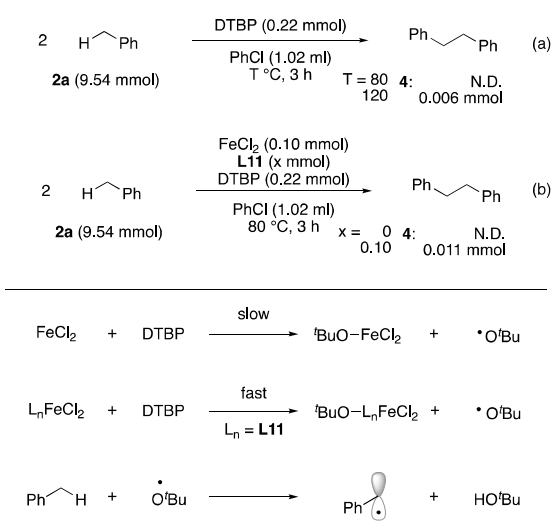

2-2. UV-Vis Spectrum Measurements

To gain insight into in situ-generated iron species, we performed UV-Vis spectrum measurements. Iron(III) chloride affords $L_nFeCl_2^+$ and $FeCl_4^-$ species in a Lewis basic solvent such as acetonitrile (eq. 1).[23]

$$2\ FeCl_3 + n\ CH_3CN \longrightarrow [Fe(CH_3CN)_nCl_2]^+[FeCl_4]^- \quad \text{(eq. 1)}$$

We first confirmed the characteristic absorptions derived from $FeCl_4^-$, as shown in Figure 1. When $FeCl_3$ was dissolved in non-coordinative dichloroethane (DCE), no characteristic absorptions derived from $FeCl_4^-$ ions were observed (Figure 1a). On the other hand, the characteristic absorptions derived from $FeCl_4^-$ ions were observed in acetonitrile at around 312 and 360 nm, indicating the generation of an enhanced Lewis acidic $L_nFeCl_2^+$ species (Figure 1b). The premixed solution of $FeCl_2$ with DTBP in chlorobenzene provided similar absorptions to the $FeCl_3$ in acetonitrile, suggesting that ^{t}BuO-$FeCl_2$ would also generate ^{t}BuO-L_nFeCl^+ and ^{t}BuO-$FeCl_3^-$ species (Figure 1c).

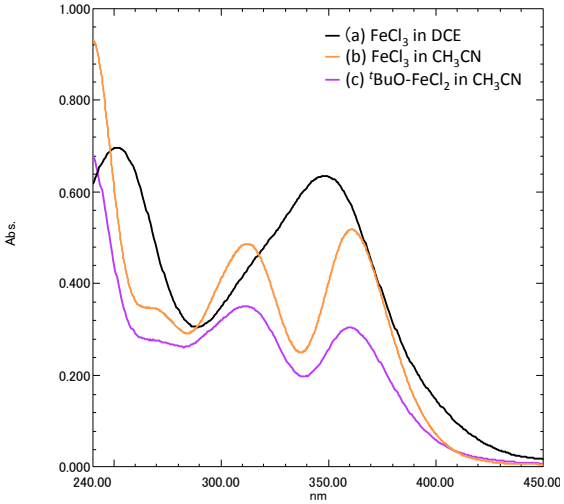

Figure 1. UV-Vis Spectroscopic Analysis of $FeCl_3$ in different solvent (a) $FeCl_3$ in DCE (black line). (b) $FeCl_3$ in CH_3CN (orange line). (c) ^{t}BuO-$FeCl_2$ in CH_3CN ($FeCl_2$ and DTBP were stirred in PhCl for 4 h at 120 °C. After removal of PhCl, resulting mixture was heated in CH_3CN for 1 h at 80 °C) (purple line)

Due to the low solubility of ^{t}BuO-$FeCl_2$ prepared from $FeCl_2$ with DTBP in chlorobenzene, further studies were conducted using $FeCl_3$ (Figure 2). As a control, phosphine oxide **L11** and acylimidazole **1a** in DCE were used respectively, and no absorption around 300-400 nm was observed (Figure 2a, 2b). The mixed solution of $FeCl_3$ with **L11** did not provide the characteristic absorptions derived from $FeCl_4^-$ ions, suggesting that **L11** would not generate $L_nFeCl_2^+$ species (Figure 2c). In contrast, the mixed solution of $FeCl_3$ with 2-acylimidazole **1a** provided absorptions derived from $FeCl_4^-$ ions (Figure 2d), suggesting that the combined use of both $FeCl_3$ and **1a** would generate $L_nFeCl_2^+$ species. We also confirmed the generation of $FeCl_4^-$ species by ESI-mass analysis (Figure S11). Furthermore, the premixed solution of $FeCl_3$ with acylimidazole **1a** and **L11** provided absorptions derived from $FeCl_4^-$ ions (Figure 2e), although the absorptions were weaker than that without **L11** (Figure 2d). These results indicated that **L11** slightly disturbs the coordination of **1a** to iron catalysts. This assumption is also consistent with the findings that the use of an increased amount of ligand **L11** decreased the chemical yield (Table 1, entry 15).

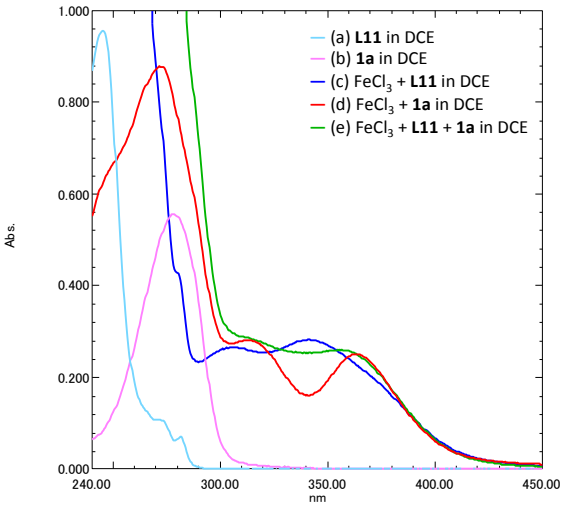

Figure 2. UV-Vis spectrum of iron catalysts (a) phosphine oxide **L11** in DCE (light blue line). (b) 2-acylimidazole **1a** in DCE (pink line). (c) $FeCl_3$ with **L11** in DCE (blue line) (d) $FeCl_3$ with 2-acylimidazole **1a** (red line) (e) $FeCl_3$ with 2-acylimidazole **1a** and **L11** in DCE (green line)

Scheme 4. Kinetic Isotope Effect

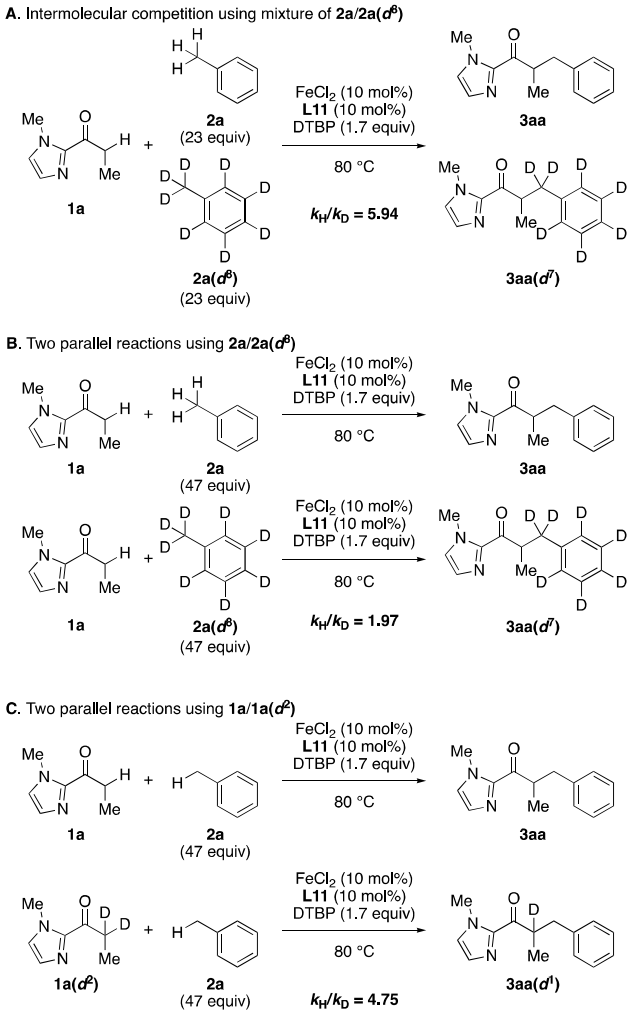

2-3. Kinetic Isotope Effect Studies and Kinetic Studies

To obtain mechanistic insight into the turnover-limiting step, a series of kinetic isotope effect (KIE) studies were performed (Scheme 4).[24] A competitive KIE study using a mixture of **2a**/**2a(*d*^{8})** revealed a large KIE value (k_H/k_D = 5.94) (Scheme 4A). On the other hand, no significant KIE was observed (k_H/k_D = 1.97), when the two parallel reactions were performed under optimized conditions using **2a** or **2a(*d*^{8})** (Scheme 4B). These results suggest that the C–H bond cleavage step of toluene has only minor contribution to the turnover-limiting and the overall rate of the reaction. In sharp contrast, relatively large KIE (k_H/k_D = 4.75) was observed from two parallel reactions using **1a**/**1a(*d*^{2})** (Scheme 4C), indicating that enolization of 2-acylimidazole has major contribution to the turnover-limiting and occur in the turnover-limiting transition state.[7b,24f]

The initial-rate kinetic study of the reaction of **1a** and **2a** was performed next to gain further information about the reaction mechanism. The reaction profiles of the present catalytic dehydrogenative coupling are summarized in Table 3.

Table 3. Kinetic Profile of the Catalytic Dehydrogenative Benzylation of 2-Acylimidazoles 1a

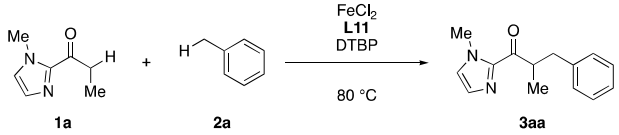

	order
catalyst ($FeCl_2$/**L11**)	2 nd
2-acylimidazole (**1a**)	zeroth
DTBP	zeroth

The reaction rate displayed second-order dependency on the catalyst ($FeCl_2$/**L11**), almost zeroth order dependency on 2-acylimidazole **1a** and DTBP. The nearly second-order kinetic dependence with respect to the catalyst suggests that two iron species would be involved in turnover-limiting step, enolization of 2-acylimidazole.[25] These result and UV-Vis spectroscopic analysis (Figure 2) and ESI-mass analysis (Figure S11) suggest that Lewis acid/Brønsted base dual activation of 2-acylimidazole **1a** by the two iron species would be operative, as depicted in Scheme 5.

Scheme 5. Dual Activation Mode of 2-Acylimidazole by Two Iron Complex

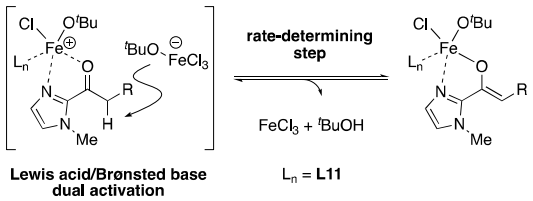

2-4. Enolate-Radical Pathway vs Radical-Radical Pathway

To elucidate whether C–C bond formation proceeded with radical-enolate coupling or radical-radical coupling, we conducted a series of control experiments (Scheme 6).[26] When the premixed catalyst prepared from $FeCl_2$ with DTBP was subjected to the reaction with benzaldehyde (**5**), aldol product **6** was observed in 22% yield with a small amount of dehydrated product, suggesting in-situ enolate formation of **1a** (Scheme 7a). Cyclopropyl-substituted 2-acylimidazole **1b** as a substrate for the radical clock experiment afforded the benzylated product **3ba** in 79% yield without any ring-opened products (Scheme 7b).[27] In addition, no dimerization of **1a** was observed using premixed catalyst prepared from $FeCl_2$ with DTBP, suggesting that an enolate-radical coupling pathway would be operative rather than a radical-radical coupling pathway (Scheme 7c).

Scheme 6. Enolate-Radical Pathway vs Radical-Radical Pathway

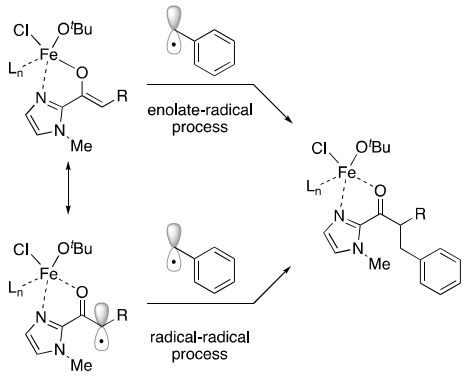

Scheme 7. Detection of 2-Acylimidazole-Derived Enolate

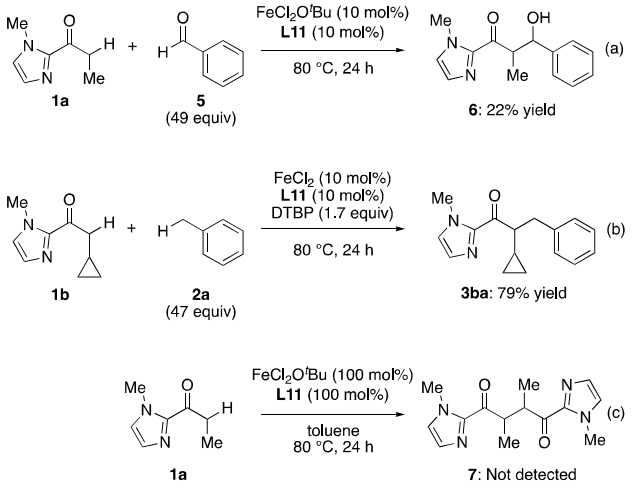

2-5. Proposed Catalytic Cycle

Mechanistic insights based on the obtained results are summarized as follows.

1. Ligand **L11** facilitates the generation of *tert*-butoxy radicals from iron(II) and DTBP, achieving efficient C–H bond cleavage of toluene under mild conditions.
2. Lewis basic 2-acylimidazoles generate the $FeCl_2^+$ and $FeCl_4^-$ species.
3. The turnover-limiting step is enolization of 2-acylimidazole and dual activation by iron species is achieved in enolization.
4. Enolate-radical coupling is operative in the C–C bond forming step.

Based on a series of mechanistic studies, a plausible catalytic cycle is depicted in Figure 3. First, iron(III) species **I** would be generated from $FeCl_2$ and DTBP through a Fenton-type reaction with the assistance of **L11**. 2-Acylimidazole **1a** coordinates to the iron catalyst, affording $Fe(III)^+$ and $Fe(III)^-$ species **II**. The enolization step involves two iron species as a Lewis acid/Brønsted base cooperative catalyst, affording enolate form **III** and radical form **IV**.[26] Benzyl C–H bond ($PhCH_2$–H: BDE = 89.8 ± 0.6 kca/mol) cleavage is achieved by *tert*-butoxy radicals (^{t}BuO–H: BDE = 105.7 ± 0.7 kcal/mol) whose generation is controlled by Fe(II)/**L11**, not by thermal heating.[27] The benzyl radical **V** couples with enolate **III** rather than radical intermediate **IV** to afford intermediate **VI**. Oxidation of iron(II) was again facilitated by **L11**, providing product **3aa** with regeneration of the active iron species **I**.

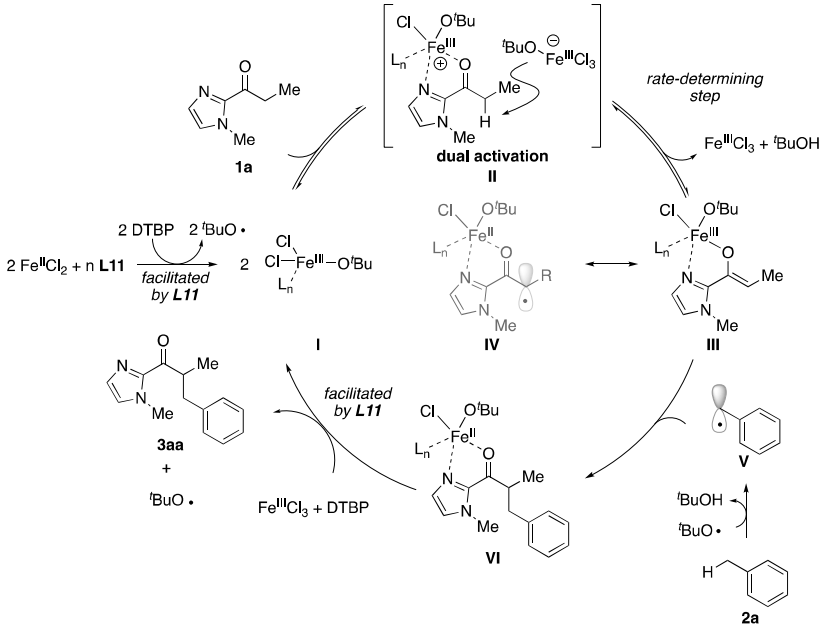

Figure 3. Proposed Catalytic Cycles

3. Reaction Scope

We investigated the scope of the iron-catalyzed dehydrogenative coupling (Table 4). Product **3aa** was isolated in 64% yield using reduced amount of toluene (15 equivalents) under 3 mol% catalyst. The gram-scale reaction also proceeded without any detrimental effects and product **3aa** was isolated in 3.94 g. Various xylenes were applicable to the present catalysis (**3ab**–**3ad**). The reactions of 4- and 3-bromotoluenes afforded the products in high yield (**3ae** and **3af**), although 2-bromotoluene afforded the product **3ag** in moderate yield, presumably due to the steric hindrance. Other arylhalides, chloro- and iodo-toluenes, afforded the product in high yield (**3ah** and **3ai**). Electron-rich methylarene was applicable, although the chemical yield was moderate (**3aj**). Base-sensitive substrates having *p*-acetoxy and methoxycarbonyl groups afforded the product at high temperature without **L11** (**3ak** and **3al**). 2,5-Dimethyl thiophene was incorporated into 2-acylimidazole in high yield (**3am**). A secondary benzylic substrate including 3-chloro-1-phenylpropane, which has additional electrophilic sites, selectively reacted at a benzylic position (**3an** and **3ao**).

Table 4. Substrate Scope of Alkylarenes[a]

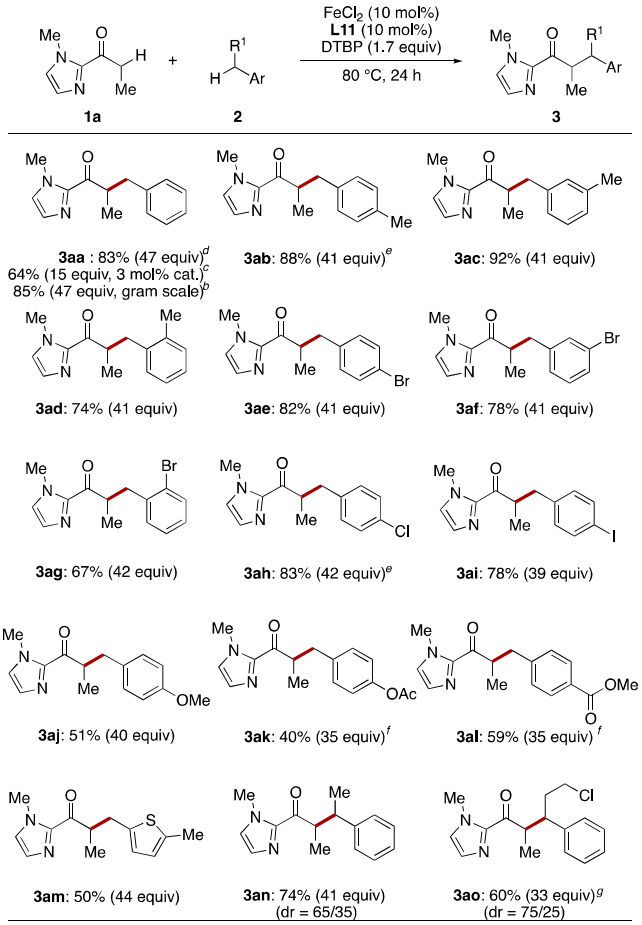

[a]Conditions: **1** (0.23 mmol), **2** (1.14 ml), 24 h. Isolated yields were shown. [b]Reaction time was 8 h. [c]3 mol% catalyst and 15 equiv of

toluene was used for 48 h. [d]3.94 g of **3aa** was isolated. [e]Reaction was performed at 90 °C. [f]Reaction was performed at 120 °C using 3.3 equiv of DTBP without **L11** [g]Yield was determined by ^{1}H-NMR analysis using 1,2,4,5-Tetramethylbenzene as an internal standard.

Next, we examined various 2-acylimidazoles (Table 5). A cyclopropyl-substituted substrate afforded product **3ba** in high yield without forming ring-opened products. A benzyl-substituted substrate was selectively benzylated in high yield (**3ca**). Terminal alkene survived under the optimized conditions (**3da**). A sterically congested substrate was applicable to the present catalysis (**3ea**). Although protecting group-free hydroxy groups terminated the catalysis, TBS-protected hydroxy groups had no detrimental effects (**3fa**). α-Phenyl and 3-thienyl 2-acylimidazole afforded the products **3ga** and **3ha** in moderate yield. *N*-Boc glycine-attached substrate was smoothly converted to benzylated product **3ia**. It is noteworthy the further functional group tolerance was demonstrated using complex molecules, such as important pharmaceuticals, indomethacin, febuxostat and telmisartan, attached-2-acylimidazoles (**3ja-3la**).

Table 5. Substrate Scope of 2-Acylimidazoles[a]

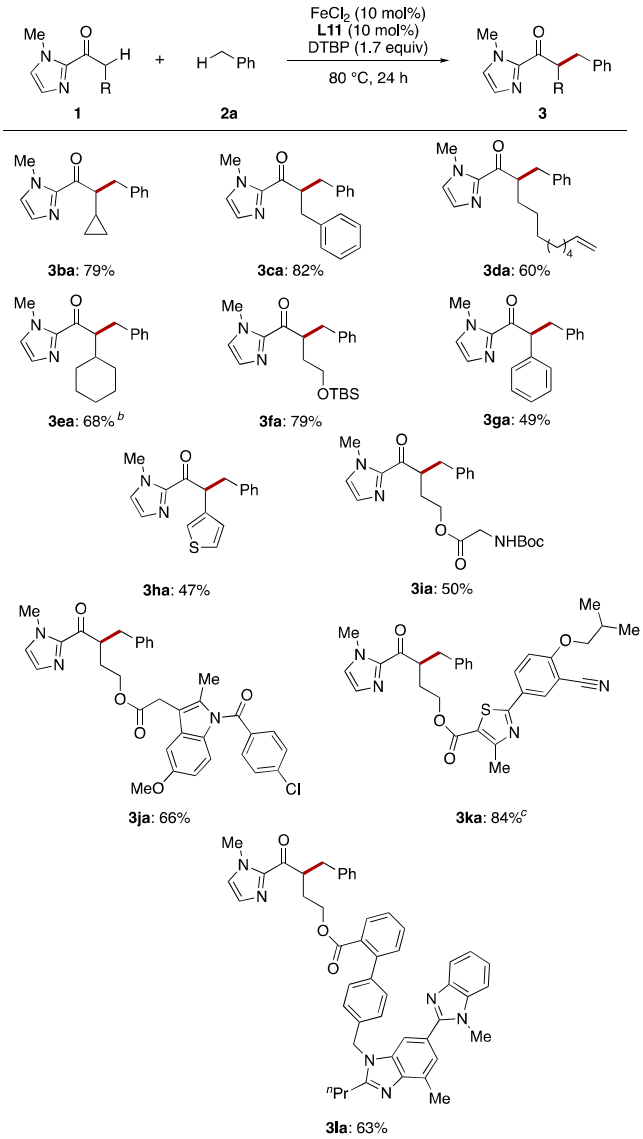

[a]Conditions: **1** (0.20 mmol), **2** (1.0 ml, 47 equiv), 24 h. Isolated yields were shown. [b]Reaction was performed at 100 °C. [c]Reaction concentration was 0.10 M.

Conventional alkylation of carbonyls using alkyl halides for the construction of an all-carbon quaternary center, is difficult due to the steric repulsion of bulky coupling partners.[14] The present dehydrogenative catalysis enabled the construction of all-carbon quaternary centers (Scheme 8). Coupling cumene and 2-bromocumene with 2-acylimidazole **1g** afforded **8** and **9**, respectively, in moderate yield. α,α-Disubstituted 2-acylimidazole **1m** was also applicable (**10**). Furthermore, the construction of contiguous all-carbon quaternary centers was achieved (**11**), and this is the first example of the construction of contiguous all-carbon quaternary centers in catalytic dehydrogenative coupling of carbonyls.

Scheme 8. Construction of All-Carbon Quaternary Center[a]

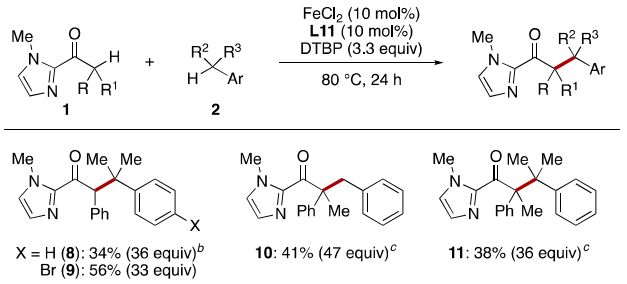

[a]Conditions: **1** (0.20 mmol), **2** (1.0 ml), 24 h. Isolated yields were shown. [b]1.7 equiv of DTBP was used. [c]Reaction was performed at 120 °C without **L11**

Scheme 9. Chemoselective Dehydrogenative Cross Coupling in the Presence of Other Enolizable Carbonyls

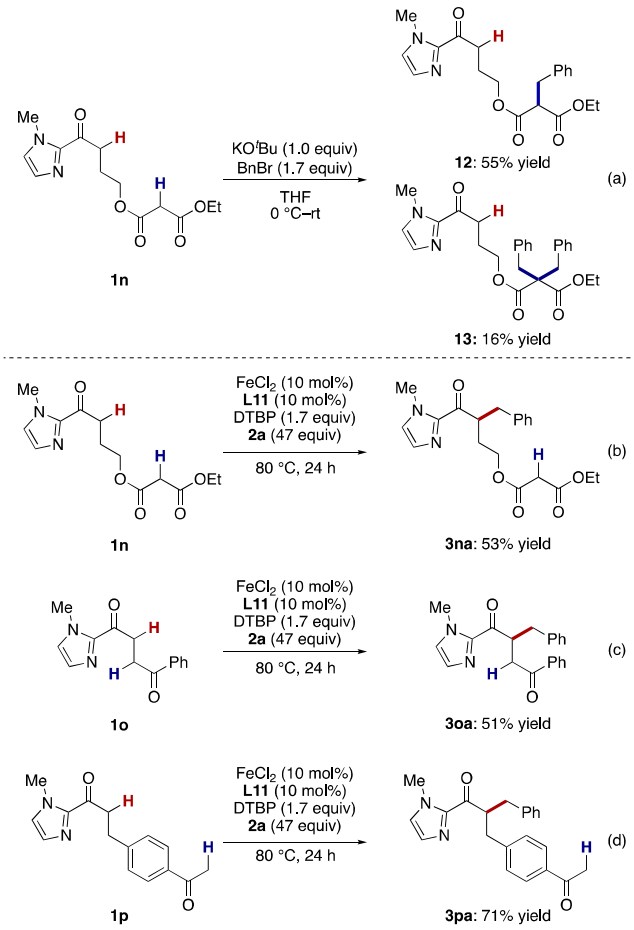

Key to the present catalysis is the combined use of an iron catalyst with Lewis basic 2-acylimidazoles, enabling efficient enolization of 2-acylimidazole through dual iron species (see, section 2-2). We envisioned that 2-acylimidazole would be chemoselectively activated even in the presence of more acidic carbonyls. Malonate diester exhibits quite high acidity (diethyl malonate; pK_a = 16.4 in DMSO, propiophenone; pK_a = 24.4 in DMSO).[29] Furthermore, the bidentate coordinative nature of the malonate diester makes chemoselective enolization of a less acidic functionality extremely difficult. Thus, we first checked the coordination ability of 2-acylimidazole and malonate diester using the UV-Vis spectrum (Figure 4). As described in section 2-2, a mixed solution of $FeCl_3$ and 2-acylimidazole **1a** provided $FeCl_4^-$ ion characteristic absorptions around 312 and 360 nm, suggesting the generation of the $L_nFeCl_2^+$ species (Figure 4b). In contrast, the mixed solution of $FeCl_3$ with diethyl malonate did not provide the characteristic absorptions derived from $FeCl_4^-$ ions (Figure 4c) and similar absorption as the $FeCl_3$ solution (Figure 4a) was observed. In addition, the premixed solution of $FeCl_3$ with 2-acylimidazole **1a** and diethyl malonate provided characteristic absorptions derived from $FeCl_4^-$ ions (Figure 4d), suggesting that 2-acylimidazole could preferentially coordinate with $L_nFeCl_2^+$ species even in the presence of bidentate coordinative diethyl malonate.

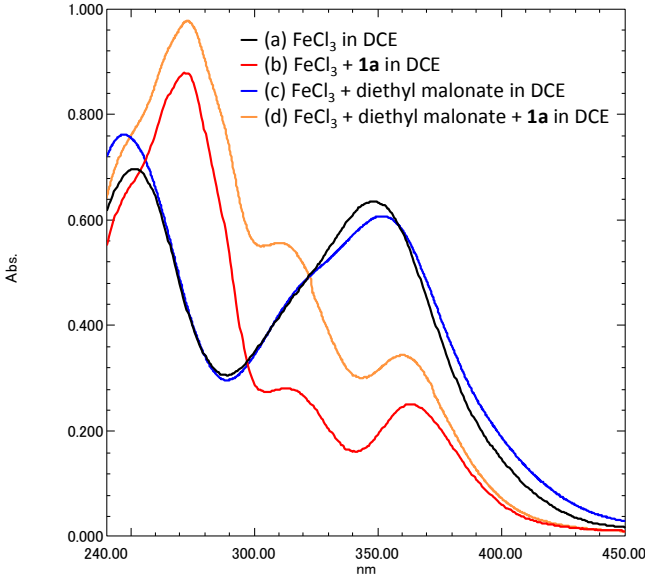

Figure 4. UV-Vis spectrum of iron catalysts (a) $FeCl_3$ in DCE (black line). (b) $FeCl_3$ with 2-acylimidazole **1a** in DCE (red line) (c) $FeCl_3$ with diethyl malonate in DCE (blue line) (d) $FeCl_3$ with 2-acylimidazole **1a** and diethyl malonate in DCE (orange line)

Based on these results, we examined **1n** bearing malonate diester as a challenging substrate for chemoselective reaction. First, to confirm the innate reactivity of the two functional groups, **1n** was subject to the conventional benzylation conditions using KO^{t}Bu and benzyl bromide (Scheme 9a). Under conventional conditions, malonate diester was benzylated exclusively and benzylated product **12** was observed with concomitant formation of di-benzylated product **13**, clearly indicating that the α-proton of the malonate functionality is innately much more acidic than the corresponding α-proton of 2-acylimidazole. In stark contrast, the 2-acylimidazole functionality was chemoselectively benzylated under the optimized iron-catalyzed conditions (Scheme 9b). Chemoselective benzylation of 1,4-diketone **1o** was achieved under the optimized conditions and product **3oa** was isolated in 51% yield (Scheme 9c). An aryl methyl ketone functionality was also applicable (Scheme 9d).

We next applied the present catalytic dehydrogenative coupling reaction to other substrates (Scheme 10). Cyclohexane (**14**) and anisole (**16**) could be used as alkylating agents, although the yields were not high.[30] Catalytic cross-oxidative enolate coupling of two distinct carboxylic acid equivalents was one of the most challenging reactions.[26,31] Acetonitrile is a fascinating carboxylic acid equivalent because it is readily available and transforms into versatile functional groups, although the bond dissociation energy of the α-C–H bond is relatively high (BDE = 96 kcal/mol).[32] In previous reports, α-radicals derived from alkyl nitriles efficiently coupled with sp^2 carbons, including those of tautomerized 1,3-ketoesters, under catalytic conditions.[33] When acetonitrile was used instead of toluene under slightly modified conditions, the cross-coupling reaction with **1a** proceeded smoothly and the cross-coupling product derived from distinct two carboxylic acid equivalents **19** was isolated in 53% yield.

Scheme 10. Dehydrogenative Cross Coupling using 2-Acylimidazole 1a

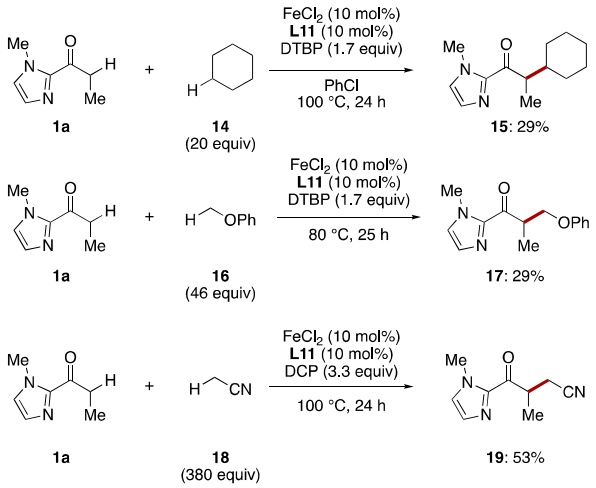

4. Transformation of the Product

Finally, the utility of the present iron catalysis was demonstrated by further elaboration of the 2-acylimidazole functionality (Scheme 11).[34] The 2-acylimidazole functionality was efficiently transformed into the corresponding carboxylic acid upon treatment with MeOTf followed by the addition of H_2O and DBU, affording **20** in high yield. The use of BnOH instead of H_2O provided benzyl ester **21** in high yield.

Conclusion

In conclusion, we developed a highly chemoselective iron-catalyzed dehydrogenative cross-coupling using 2-acylimidazoles and alkylarenes. Mechanistic studies revealed the role of phosphine oxide **L11**, and dual activation of 2-acylimidazoles by two iron species was also elucidated. Various alkylarenes, aliphatic alkane, acetonitrile, and functionalized 2-acylimidazole can be used under mild conditions. Furthermore, contiguous all-carbon quaternary centers were constructed through dehydrogenative cross-coupling for the first time. It is also noteworthy that 2-acylimidazole was chemoselectively activated, even in the presence of bidentate coordinative and much more acidic malonate diester.

Scheme 11. Transformation of the 2-Acylimidazole

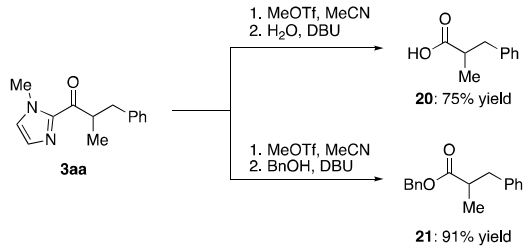

ASSOCIATED CONTENT

Supporting Information

The supporting information is available free of charge on the ACS Publications website at DOI:

Detailed experimental procedures and spectroscopic data for all new compounds (PDF).

AUTHOR INFORMATION

Corresponding Author

*yazaki@phar.kyushu-u.ac.jp
*ohshima@phar.kyushu-u.ac.jp

Notes

The authors declare no competing financial interest.

ACKNOWLEDGMENT

This work was financially supported by JSPS KAKENHI Grant Number JP15H05846 in Middle Molecular Strategy, JP16H01032 in Precisely Designed Catalysts with Customized Scaffolding, Grant-in-Aid for Scientific Research (C) (#16K08166) and Platform Project for Supporting Drug Discovery and Life Science Research (Basis for Supporting Innovative Drug Discovery and Life Science Research (BINDS)) from AMED under Grant Number JP17am0101091. R.Y. thanks the Sumitomo Foundation for financial support.

REFERENCES

(1) Recent reviews on C-H cross coupling reactions, see: (a) Ritleng, V.; Sirlin, C.; Pfeffer, M. Ru-, Rh-, and Pd-Catalyzed C−C Bond Formation Involving C−H Activation and Addition on Unsaturated Substrates: Reactions and Mechanistic Aspects. *Chem. Rev.* **2002**, *102*, 1731-1770. (b) Li, Z.; Li, C.-J. Highly Efficient Copper-Catalyzed Nitro-Mannich Type Reaction: Cross-Dehydrogenative-Coupling between sp^3 C−H Bond and sp^3 C−H Bond. *J. Am. Chem. Soc.* **2005**, *127*, 3672-3673. (c) Li, C.-J. Cross-Dehydrogenative Coupling (CDC): Exploring C−C Bond Formations beyond Functional Group Transformations. *Acc. Chem. Res.* **2009**, *42*, 335-344. (d) Liu, C.; Zhang, H.; Shi, W.; Lei, A. Bond Formations between Two Nucleophiles: Transition Metal Catalyzed Oxidative Cross-Coupling

Reactions. *Chem. Rev.* **2011**, *111*, 1780-1824. (e) Girard, S. A.; Knauber, T.; Li, C.-J. The Cross-Dehydrogenative Coupling of Csp3-H Bonds: A Versatile Strategy for C-C Bond Formations. *Angew. Chem. Int. Ed.* **2014**, *53*, 74-100. (f) Kozlowski, M. C. *Acc. Chem. Res.* **2017**, *50*, 638-643. (g) Lv, L. Y.; Li, Z. P. Fe-Catalyzed Cross-Dehydrogenative Coupling Reactions. *Top. Curr. Chem.* **2016**, *374*, 38-39.

(2) (a) Davies, H. M. L.; Hansen, T. Asymmetric Intermolecular Carbenoid C−H Insertions Catalyzed by Rhodium(II) (*S*)-*N*-(*p*-Dodecylphenyl)sulfonylprolinate. *J. Am. Chem. Soc.* **1997**, *119*, 9075-9076. (b) Waltz, K. M.; Hartwig, J. F. Functionalization of Alkanes by Isolated Transition Metal Boryl Complexes. *J. Am. Chem. Soc.* **2000**, *122*, 11358-11369. (c) Chen, M. S.; White, M. C. A Predictably Selective Aliphatic C–H Oxidation Reaction for Complex Molecule Synthesis. *Science* **2007**, *318*, 783-787. (d) Yeung, C. S.; Dong, V. M. Catalytic Dehydrogenative Cross-Coupling: Forming Carbon−Carbon Bonds by Oxidizing Two Carbon−Hydrogen Bonds. *Chem. Rev.* **2011**, *111*, 1215-1292. (e) Curto, J. M.; Kozlowski, M. C. Chemoselective Activation of sp^3 vs sp^2 C–H Bonds with Pd(II). *J. Am. Chem. Soc.* **2015**, *137*, 18-21. (f) Vanjari, R.; Singh, K. N. Utilization of Methylarenes as Versatile Building Blocks in Organic Synthesis. *Chem. Soc. Rev.* **2015**, *44*, 8062-8096. (g) Banerjee, A.; Sarkar, S.; Patel, B. K. C–H Functionalisation of Cycloalkanes. *Org. Biomol. Chem.* **2017**, *15*, 505-530.

(3) (a) Yao, Z.; Klabunde, K. J. The Strong Acidity and the Process for Deprotonation of $(\eta^6\text{-Toluene})Fe(H)_2(SiCl_3)_2$. *Inorg. Chem.* **1997**, *36*, 2119-2123. (b) Mao, J.; Zhang, J.; Jiang, H.; Bellomo, A.; Zhang, M.; Gao, Z.; Dreher, S. D.; Walsh, P. J. Palladium-Catalyzed Asymmetric Allylic Alkylations with Toluene Derivatives as Pronucleophiles. *Angew. Chem. Int. Ed.* **2016**, *55*, 2526-2530.

(4) (a) Liu, C.; Liu, D.; Lei, A. Recent Advances of Transition-Metal Catalyzed Radical Oxidative Cross-Couplings. *Acc. Chem. Res.* **2014**, *47*, 3459-3470. (b) Yan, M.; Lo, J. C.; Edwards, J. T.; Baran, P. S. Radicals: Reactive Intermediates with Translational Potential. *J. Am. Chem. Soc.* **2016**, *138*, 12692-12714. (c) Yi, H.; Zhang, G.; Wang, H.; Huang, Z.; Wang, J.; Singh, A. K.; Lei, A. Recent Advances in Radical C–H Activation/Radical Cross-Coupling. *Chem. Rev.* **2017**, *117*, 9016-9085.

(5) Claridge, R. F. C.; Fischer, H. Self-termination and electronic spectra of substituted benzyl radicals in solution. *J. Phys. Chem.* **1983**, *87*, 1960-1967.

(6) Coupling with sp^2 carbon, see (a) Zhao, J.; Fang, H.; Qian, P.; Han, J.; Pan, Y. Metal-Free Oxidative $C(sp^3)$–H Bond Functionalization of Alkanes and Conjugate Addition to Chromones. *Org. Lett.* **2014**, *16*, 5342-5345. (b) Zhou, S. L.; Guo, L. N.; Wang, H.; Duan, X. H. Copper□Catalyzed Oxidative Benzylarylation of Acrylamides by Benzylic C−H Bond Functionalization for the Synthesis of Oxindoles. *Chem. Eur. J.* **2013**, *19*, 12970-12973. (c) Zhao, J.; Fang, H.; Song, R.; Zhou, J.; Han, J.; Pan, Y. Metal-Free Oxidative $C(sp^3)$-H Bond Functionalization of Alkanes and Alkylation-Initiated Radical 1,2-Aryl Migration in α,α-Diaryl Allylic Alcohols. *Chem. Commun.* **2015**, *51*, 599-602. (d) Wan, M.; Lou, H.; Liu, L. C_1-Benzyl and Benzoyl Isoquinoline Synthesis through Direct Oxidative Cross-Dehydrogenative Coupling with Methyl Arenes. *Chem. Commun.* **2015**, *51*, 13953-13956. (e) Qin, G.; Chen, X.; Yang, L.; Huang, H. Copper-Catalyzed α-Benzylation of Enones via Radical-Triggered Oxidative Coupling of Two C–H Bonds. *ACS Catal.* **2015**, *5*, 2882-2885. (f) Li, G.; Li, D.; Zhang, J.; Shi, D. Q.; Zhao, Y. Ligand-Enabled Regioselectivity in the Oxidative Cross-coupling of Arenes with Toluenes and Cycloalkanes Using Ruthenium Catalysts: Tuning the Site-Selectivity from the *ortho* to *meta* Positions. *ACS Catal.* **2017**, *7*, 4138-4143. (g) Li, B.; Fang, S. L.; Huang, D. Y.; Shi, B. F. Ru-Catalyzed *Meta*-C–H Benzylation of Arenes with Toluene Derivatives. *Org. Lett.* **2017**, *19*, 3950. (h) Soni, V.; Khake, S. M.; Punji, B. Nickel-Catalyzed $C(sp^2)$–H/$C(sp^3)$–H Oxidative Coupling of Indoles with Toluene Derivatives. *ACS Catal.* **2017**, *7*, 4202-4208. (i) Zhou, R.; Liu, H.-W.; Tao, H.-R.; Yu, X.-J.; Wu, J. Metal-Free Direct Alkylation of Unfunctionalized Allylic/Benzylic sp^3 C−H Bonds via Photoredox Induced Radical Cation Deprotonation. *Chem. Sci.* **2017**, *8*, 4654−4659. (j) Liu, H.; Ma, L.; Zhou, R.; Chen, X.; Fang, W.; Wu, J. One-Pot Photomediated Giese Reaction/Friedel–Crafts Hydroxyalkylation/Oxidative Aromatization To Access Naphthalene Derivatives from Toluenes and Enones. *ACS Catal.* **2018**, *8*, 6224-6229. (k) Mazzarella, D.; Crisenza, G. E. M.; Melchiorre, P. Asymmetric Photocatalytic C−H Functionalization of Toluene and Derivatives. *J. Am. Chem. Soc.* **2018**, *140*, 8439.

(7) Coupling with organometallic reagent, see (a) Liu, D.; Li, Y.; Qi, X.; Liu, C.; Lan, Y.; Lei, A. Nickel-Catalyzed Selective Oxidative Radical Cross-Coupling: An Effective Strategy for Inert Csp^3–H Functionalization. *Org. Lett.* **2015**, *17*, 998-1001. (b) Zhang, W.; Wang, F.; McCann, S. D.; Wang, D.; Chen, P.; Stahl, S. S.; Liu, G. Enantioselective Cyanation of Benzylic C–H Bonds via Copper-Catalyzed Radical Relay. *Science,* **2016**, *353*, 1014-1018. (c) Vasilopoulos, A.; Zultanski, S. L.; Stahl, S. S. Feedstocks to Pharmacophores: Cu-Catalyzed Oxidative Arylation of Inexpensive Alkylarenes Enabling Direct Access to Diarylalkanes. *J. Am. Chem. Soc.* **2017**, *139*, 7705-7708. (d) Zhang, W.; Chen, P.; Liu, G. Copper-Catalyzed Arylation of Benzylic C–H bonds with Alkylarenes as the Limiting Reagents. *J. Am. Chem. Soc.* **2017**, *139*, 7709-7712.

(8) Recent examples of coupling reaction with heteroatoms, see (a) Pelletier, G.; Powell, D. A. Copper-Catalyzed Amidation of Allylic and Benzylic C-H Bonds. *Org. Lett.* **2006**, *8*, 6031-6034. (b) Xia, Q.; Chen, W.; Qiu, H. Direct C–N Coupling of Imidazoles and Benzylic Compounds via Iron-Catalyzed Oxidative Activation of C–H Bonds. *J. Org. Chem.* **2011**, *76*, 7577-7582. (c) Gephart, R. T., III; McMullin, C. L.; Sapiezynski, N. G.; Jang, E. S.; Aguila, M. J. B.; Cundari, T. R.; Warren, T. H. Reaction of Cu^I with Dialkyl Peroxides: Cu^{II}-Alkoxides, Alkoxy Radicals, and Catalytic C–H Etherification. *J. Am. Chem. Soc.* **2012**, *134*, 17350-17353. (d) Liu, H.; Shi, G.; Pan, S.; Jiang, Y.; Zhang, Y. Palladium-Catalyzed Benzylation of Carboxylic Acids with Toluene via Benzylic C–H Activation. *Org. Lett.* **2013**, *15*, 4098-4101. (e) Tran, B. L.; Driess, M.; Hartwig, J. F. Copper-Catalyzed Oxidative Dehydrogenative Carboxylation of Unactivated Alkanes to Allylic Esters via Alkenes. *J. Am. Chem. Soc.* **2014**, *136*, 17292-17301. (f) Tran, B. A.; Li, B.; Driess, M.; Hartwig, J. F. Copper-Catalyzed Intermolecular Amidation and Imidation of Unactivated Alkanes. *J. Am. Chem. Soc.* **2014**, *136*, 2555-2563. (g) García-Cabeza, A. L.; Marín-Barrios, R.; Moreno-Dorado, F. J.; Ortega, M. J.; Massanet, G. M.; Guerra, F. M. Allylic Oxidation of Alkenes Catalyzed by a Copper–Aluminum Mixed Oxide. *Org. Lett.* **2014**, *16*, 1598-1601. (h) Cheng, Y.; Dong, W.; Wang, L.; Parthasarathy, K.; Bolm, C. Iron-Catalyzed Hetero-Cross-Dehydrogenative Coupling Reactions of Sulfoximines with Diarylmethanes: A New Route to *N*-Alkylated Sulfoximines. *Org. Lett.* **2014**, *16*, 2000-2002. (i) Zhou, L.; Tang, S.; Qi, X.; Lin, C.; Liu, K.; Liu, C.; Lan, Y.; Lei, A. Transition-Metal-Assisted Radical/Radical Cross-Coupling: A New Strategy to the Oxidative $C(sp^3)$–H/N–H Cross-Coupling. *Org. Lett.* **2014**, *16*, 3404-3407. (j) Zeng, H.-T.; Huang, J.-M. Copper-Catalyzed Ligand-Free Amidation of Benzylic Hydrocarbons and Inactive Aliphatic Alkanes. *Org. Lett.* **2015**, *17*, 4276-4279. (k) Chikkade, P. K.; Kuninobu, Y.; Kanai, M. Copper-Catalyzed Intermolecular $C(sp^3)$–H Bond Functionalization towards the Synthesis of Tertiary Carbamates. *Chem. Sci.* **2015**, *6*, 3195-3200. (l) He, Y.; Mao, J.; Rong, G.; Yan, H.; Zhang, G. Iron- Catalyzed Esterification of Benzyl C−H Bonds to Form α- Keto Benzyl Esters. *Adv. Synth. Catal.* **2015**, *357*, 2125-2131. (m) Rabet, P. T. G.; Fumagalli, G.; Boyd, S.; Greaney, M. F. Benzylic C–H Azidation Using the Zhdankin Reagent and a Copper Photoredox Catalyst. *Org. Lett.* **2016**, *18*, 1646-1649. (n) Ren, T. L.; Xu, B. H.; Mahmood, S.; Sun, M. X.; Zhang, S. J. Cobalt-Catalyzed Oxidative Esterification of Allylic/Benzylic $C(sp^3)$-H Bonds. *Tetrahedron* **2017**, *73*, 2943-2948. (o) Lu, B.; Zhu, F.; Sun, H. M.; Shen, Q. Esterification of the Primary Benzylic C–H Bonds with Carboxylic Acids Catalyzed by Ionic Iron(III) Complexes Containing an Imidazolinium Cation. *Org. Lett.* **2017**, *19*, 1132-1135. For reviews, also see (p) Guntreddi, T.; Vanjari, R.; Singh, K. N. Direct conversion of methylarenes into dithiocarbamates, thioamides and benzyl esters. *Tetrahedron* **2014**, *70*, 3887-3892. (q) Majji, G.; Rout, S. K.; Rajamanickam, S.; Guin, S.; Patel, B. K. Synthesis of Esters via sp^3 C–H Functionalisation. *Org. Biomol. Chem.* **2016**, *14*, 8178-8211.

(9) Directing group-assisted Csp^3-Csp^3 dehydrogenative cross coupling, see (a) Kubo, T.; Aihara, Y.; Chatani, N. Pd(II)-catalyzed Chelation-assisted Cross Dehydrogenative Coupling between Unactivated $C(sp^3)$–H Bonds in Aliphatic Amides and Benzylic C–H Bonds in Toluene Derivatives. *Chem. Lett*. **2015**, *44*, 1365-1367. (b) Li, K.; Wu, Q.; Lan, J.; You, J. Coordinating Activation Strategy for $C(sp^3)$–H/$C(sp^3)$–H Cross-Coupling to Access β-Aromatic α-Amino Acids. *Nat. Commun*. **2015**, *6*, 8404-8412. (c) Tan, M.; Li, K.; Yin, J.; You, J. Manganese/Cobalt-Catalyzed Oxidative $C(sp^3)$–H/$C(sp^3)$–H Coupling: A Route to α-Tertiary β-Arylethylamines. *Chem. Commun.* **2018**, *54*, 1221-1224.

(10) Directing group-assisted Csp^2-Csp^3 dehydrogenative cross coupling, see (a) Aihara, Y.; Tobisu, M.; Fukumoto, Y.; Chatani, N. Ni(II)-Catalyzed Oxidative Coupling between $C(sp^2)$–H in Benzamides and $C(sp^3)$–H in Toluene Derivatives. *J. Am. Chem. Soc*. **2014**, *136*, 15509-15512. (b) Zhang, H.-J.; Su, F.; Wen, T.-B. Copper-Catalyzed Direct C2-Benzylation of Indoles with Alkylarenes. *J. Org. Chem*. **2015**, *80*, 11322-11329. (c) Sattar, M.; Kumar, S. Palladium-Catalyzed Removable 8-Aminoquinoline Assisted Chemo- and Regioselective Oxidative sp^2-C–H/sp^3-C–H Cross-Coupling of Ferrocene with Toluene Derivatives. *Org. Lett.* **2017**, *19*, 5960-5963.

(11) Smith, M. B.; March, J. March's Advanced Organic Chemistry (Wiley, New York, 2001).

(12) Recent our contribution of catalytic chemoselective enolization, see; (a) Tanaka, T.; Tanaka, T.; Tsuji, T.; Yazaki, R.; Ohshima, T. Strategy for Catalytic Chemoselective Cross-Enolate Coupling Reaction via a Transient Homocoupling Dimer. *Org. Lett*. **2018**, *20*, 3541-3544. (b) Tokumasu, K.; Yazaki, R.; Ohshima, T. Direct Catalytic Chemoselective α-Amination of Acylpyrazoles: A Concise Route to Unnatural α-Amino Acid Derivatives. *J. Am. Chem. Soc*. **2016**, *138*, 2664-2669. (c) Taninokuchi, S.; Yazaki, R.; Ohshima, T. Catalytic Aerobic Chemoselective α-Oxidation of Acylpyrazoles en Route to α-Hydroxy Acid Derivatives. *Org. Lett*. **2017**, *19*, 3187-3190.

(13) Oettingen, W. F. The Halogenated Hydrocarbons of Industrial and Toxicological Importance. Elsevier, Amsterdam, New York, **1964**, *116*, 960-961.

(14) For reviews on construction of all-carbon quaternary center, see (a) Douglas, C. J.; Overman, L. E. Catalytic Asymmetric Synthesis of All-Carbon Quaternary Stereocenters. *Proc. Natl. Acad. Sci. USA*. **2004**, *101*, 5363-5367. (b) Peterson, E. A.; Overman, L. E. Contiguous Stereogenic Quaternary Carbons: A Daunting Challenge in Natural Products Synthesis. *Proc. Natl. Acad. Sci. USA*. **2004**, *101*, 11943-11948. (c) Trost, B. M.; Jiang, C. Catalytic Enantioselective Construction of All-Carbon Quaternary Stereocenters. *Synthesis,* **2006**, 369-396.

(15) (a) Li, Z.; Cao, L.; Li, C.-J. $FeCl_2$□Catalyzed Selective C−C Bond Formation by Oxidative Activation of a Benzylic C−H Bond. *Angew. Chem. Int. Ed.* **2007**, *46*, 6505-6507. (b) Correia, C. A.; Li, C. -J. Catalytic Alkylation of Benzylic C–H Bonds with 1,3-Dicarbonyl Compounds utilizing Oxygen as Terminal Oxidant. *Tetrahedron Lett.* **2010**, *51*, 1172-1175.

(16) (a) Zhang, Y.; Li, C.-J. Highly Efficient Direct Alkylation of Activated Methylene by Cycloalkanes. *Eur. J. Org. Chem.* **2007**, 4654-4657. (b) Borduas, N.; Powell, D. A. Copper-Catalyzed Oxidative Coupling of Benzylic C−H Bonds with 1,3-Dicarbonyl Compounds. *J. Org. Chem.* **2008**, *73*, 7822-7825. (c) Pan, S. G.; Liu, J. H.; Li, Y. M.; Li, Z. P. Iron-Catalyzed Benzylation of 1,3-Dicarbonyl Compounds by Simple Toluene Derivatives. *Chin. Sci. Bull.* **2012**, *57*, 2382-2386. (d) Yang, K.; Song, Q. Fe-Catalyzed Double Cross-Dehydrogenative Coupling of 1,3-Dicarbonyl Compounds and Arylmethanes. *Org. Lett.* **2015**, *17*, 548-551.

(17) Recently microwave assisted alkylation of acetophenone derivatives was reported. In this report, moderate yields are observed presumably due to the formation of undesired homo-coupling dimer formation under harsh reaction conditions (160 °C, excess amount of oxidant), see; Wang, Q.-Q.; Wang, Z.-X.; Zhang, X.-Y.; Fan, X.-S. Microwave□Promoted Metal□Free α□Alkylation of Ketones with Cycloalkanes through Cross□Coupling of $C(sp^3)$−H Bonds. *Asian J. Org. Chem.* **2017**, *6,* 1445-1450.

(18) Utility of 2-acylimidazoles, see: (a) Ohta, S.; Hayakawa, S.; Nishimura, K.; Okamoto, M. Synthesis and Application of Imidazole Derivatives. Synthesis of (1-Methyl-1*H*-imidazol-2-yl) methanol Derivatives and Conversion into Carbonyl Compounds. *Chem. Pharm. Bull*. **1987**, *35*, 1058-1069. (b) Evans, D. A.; Fandrick, K. R.; Song, H.-J. Enantioselective Friedel−Crafts Alkylations of α,β-Unsaturated 2-Acyl Imidazoles Catalyzed by Bis(oxazolinyl)pyridine−Scandium(III) Triflate Complexes. *J. Am. Chem. Soc*. **2005**, *127*, 8942-8943.

(19) Pioneering work of catalytic radical cross coupling reaction using 2-acylimidazoles, see; Huo, H.; Shen, X.; Wang, C.; Zhang, L.; Röse, P.; Chen, L. A.; Harms, K.; Marsch, M.; Hilt, G.; Meggers, E. Asymmetric Photoredox Transition-Metal Catalysis Activated by Visible Light. *Nature* **2014**, *515,* 100-103.

(20) (a) Lv, J.; Chen, W.; Chen, L.; Tian, Y.; Sun, X. Thermal Decomposition Analysis and Safety Study on Di-tert-butyl Peroxide. *Procedia Eng.* **2012**, *43*, 312-317.

(21) Other oxidants were not effective, see Supporting Information for details.

(22) Rachmilovich-Calis, S.; Masarwa, A.; Meyerstein, N.; Meyerstein, D.; Van Eldik, R. New Mechanistic Aspects of the Fenton Reaction. *Chem. Eur. J.* **2009**, *15*, 8303-8309.

(23) Lewis base assisted $FeCl_2^+$ generation, see: (a) Swanson, T. B.; Laurie, V. W. Electron Magnetic Resonance and Electronic Spectra of Tetrachloroferrate(III) Ion in Nonaqueous Solution. *J. Phys. Chem.* **1965**, *69*, 244-250. (b) Tobinaga, S.; Kotani, E. Intramolecular and Intermolecular Oxidative Coupling Reactions by a New Iron Complex $[Fe(DMF)_3Cl_2][FeCl_4]$. *J. Am. Chem. Soc*. **1972**, *94*, 309-310. (c) Tomifuji, R.; Kurahashi, T.; Matsubara, S. Iron Catalyzed [4+2] Cycloaddition of Imines and Dienes. 62nd Symposium on Organometallic Chemistry, Japan, Presentation number P3-17, September 7-9. (d) Tomifuji, R.; Kurahashi, T.; Matsubara, S. Asymmetric [4+2] Cycloaddition of Aldehydes with Dienes Catalyzed by Cationic Iron(III) Complex. 63rd Symposium on Organometallic Chemistry, Japan, Presentation number P3-06, September 14-16. (e) Tomifuji, R.; Kurahashi, T.; Matsubara, S. Cationic Iron(III) Complex Catalyzed Asymmetric Hetero Diels-Alder Reaction of Aldehydes with Simple Dienes. 64th Symposium on Organometallic Chemistry, Japan, Presentation number P2-99, September 7-9.

(24) (a) Wiberg, K. B. The Deuterium Isotope Effect. *Chem. Rev.* **1955**, *55*, 713-743. (b) Bell, R. P. Liversidge Lecture. Recent Advances in the Study of Kinetic Hydrogen Isotope Effects. *Chem. Soc. Rev.* **1974**, *3*, 513-544. (c) Giagou, T.; Meyer, M. P. Kinetic Isotope Effects in Asymmetric Reactions. *Chem. Eur. J.* **2010**, *16,* 10616-10628. (d) Klinman, J. P. A New Model for the Origin of Kinetic Hydrogen Isotope Effects. *J. Phys. Org. Chem*. **2010**, *23*, 606-612. (e) Kozuch, S.; Shaik, S. How to Conceptualize Catalytic Cycles? The Energetic Span Model. *Acc. Chem. Res.* **2011**, *44*, 101-110. (f) Simmons, E. M.; Hartwig, J. F. On the Interpretation of Deuterium Kinetic Isotope Effects in C−H Bond Functionalizations by Transition□Metal Complexes. *Angew. Chem. Int. Ed.* **2012**, *51*, 3066-3072.

(25) Jie, X.; Shang, Y.; Zhang, X.; Su, W. Cu-Catalyzed Sequential Dehydrogenation–Conjugate Addition for β-Functionalization of Saturated Ketones: Scope and Mechanism. *J. Am. Chem. Soc.* **2016**, *138*, 5623-5633. Also see, Shang, Y.; Jie, X.; Jonnada, K.; Zafar, S. N.; Su, W. Dehydrogenative desaturation-relay via formation of multicenter-stabilized radical intermediates. *Nat. Commun.* **2017**, *8*, 2273-2280.

(26) DeMartino, M. P.; Chen, K.; Baran, P. S. Intermolecular Enolate Heterocoupling: Scope, Mechanism, and Application. *J. Am. Chem. Soc*. **2008**, *130,* 11546-11560.

(27) Griller, D.; Ingold, K. U. Free-Radical Clocks. *Acc. Chem. Res.* **1980**, *13*, 317-323.

(28) For a review on bond dissociation energies, see (a) Blanksby, S. J.; Ellison, G. B. Bond Dissociation Energies of Organic Molecules. *Acc. Chem. Res.* **2003**, *36*, 255-263. (b) Xue, X. S.; Ji, P.; Zhou, B.; Cheng, J. P. The Essential Role of Bond Energetics in C–H Activation/Functionalization. *Chem. Rev.* **2017**, *117*, 8622-8648.

(29) Bordwell, F. G. Equilibrium Acidities in Dimethyl Sulfoxide Solution. *Acc. Chem. Res.* **1988**, *21*, 456-463.

(30) No improvement was observed at elevated reaction temperature.

(31) For reviews on oxidative cross enolate coupling, see (a) Csákÿ, A. G.; Plumet, J. Stereoselective Coupling of Ketone and Carboxylate Enolates. *Chem. Soc. Rev.* **2001**, *30*, 313-320. (b) Guo, F.; Clift, M. D.; Thomson, R. J. Oxidative Coupling of Enolates, Enol Silanes, and Enamines: Methods and Natural Product Synthesis. *Eur. J. Org. Chem.* **2012**, 4881-4896.

(32) Chu, X. Q.; Ge, D.; Shen, Z. L.; Loh, T. P. Recent Advances in Radical-Initiated C(sp^3)–H Bond Oxidative Functionalization of Alkyl Nitriles. *ACS Catal.* **2018**, *8*, 258-271.

(33) (a) Bunescu, A.; Wang, Q.; Zhu, J. Copper Mediated/Catalyzed Oxyalkylation of Alkenes with Alkylnitriles. *Chem. Eur. J.* **2014**, *20*, 14633-1436. (b) Li, J.; Wang, Z.; Wu, N.; Gao, G.; You, J. Radical Cascade Cyanomethylation of Activated Alkenes to Construct Cyano Substituted Oxindoles. *Chem. Commun.* **2014**, *50*, 15049-15051. (c) Bunescu, A.; Wang, Q.; Zhu, J. Synthesis of Functionalized Epoxides by Copper-Catalyzed Alkylative Epoxidation of Allylic Alcohols with Alkyl Nitriles. *Org. Lett.* **2015**, *17*, 1890-1893. (d) Bunescu, A.; WangDr, Q.; Zhu, J. *Angew. Chem. Int. Ed.* **2015**, *54*, 3132-3135. (e) Chatalova-Sazepin, C.; Wang, Q.; Sammis, G. M.; Zhu, J. Copper Catalyzed Intermolecular Carboetherification of Unactivated Alkenes by Alkyl Nitriles and Alcohols. *Angew. Chem. Int. Ed.* **2015**, *54*, 5443-5446. (f) Li, Z.; Xiao, Y.; Liu, Z.-Q. A Radical anti-Markovnikov Addition of Alkyl Nitriles to Simple Alkenes *via* Selective sp^3 C–H Bond Functionalization. *Chem. Commun.* **2015**, *51*, 9969-9971. (g) Pan, C.; Zhang, H.; Zhu, C. Fe-Promoted Radical Cyanomethylation/Arylation of Arylacrylamides to Access Oxindoles *via* Cleavage of the sp^3 C–H of Acetonitrile and the sp^2 C–H of the Phenyl Group. *Org. Biomol. Chem.* **2015**, *13*, 361-364. (h) Ha, T. M.; Wang, Q.; Zhu, J. Copper-Catalysed Cyanoalkylative Cycloetherification of Alkenes to 1,3-Dihydroisobenzofurans: Development and Application to the Synthesis of Citalopram. *Chem. Commun.* **2016**, *52*, 11100-11103. (i) Wang, C.; Li, Y.; Gong, M.; Wu, Q.; Zhang, J.; Kim, J. K.; Huang, M.; Wu, Y. Method for Direct Synthesis of α-Cyanomethyl-β-dicarbonyl Compounds with Acetonitrile and 1,3-Dicarbonyls. *Org. Lett.* **2016**, *18*, 4151-4153. (j) Su, H.; Wang, L.; Rao, H.; Xu, H. Iron-Catalyzed Dehydrogenative sp^3–sp^2 Coupling via Direct Oxidative C–H Activation of Acetonitrile. *Org. Lett.* **2017**, *19*, 2226-2229.

(34) Evans, D. A.; Fandick, K. R. Catalytic Enantioselective Pyrrole Alkylations of α,β-Unsaturated 2-Acyl Imidazoles. *Org. Lett.* **2006**, *8*, 2249-2252.